

## ORIGINAL ARTICLE

# Influence of Annealing Temperature on the Optical, Structural, Morphological and Compositional Properties of SILAR Deposited Copper Manganese Oxide Thin Films

N. L. Okoli<sup>a,c,\*</sup>, C. J. Nkamuo<sup>b</sup>, C. I. Elekalachi<sup>c</sup>, and I. O. Obimma<sup>b</sup>

<sup>a</sup> Department of Physics, Legacy University Okija, Anambra State, Nigeria.

<sup>b</sup> Department of Science Laboratory and Technology, Federal Polytechnic Oke, Anambra State, Nigeria.

<sup>c</sup> Department of Industrial Physics, Chukwuemeka Odumegwu Ojukwu University, Uli, Anambra State, Nigeria

## KEYWORDS

CuMnO<sub>2</sub>,  
Annealing temperature,  
SILAR cycles,  
Optical analysis,  
Crystallite sizes

## ARTICLE HISTORY

Received: May 21, 2022

Revised: June 11, 2022

Accepted: August 03, 2022

## ABSTRACT

In this work, effects of annealing temperature on the optical, structural, morphological, and compositional properties of SILAR deposited copper manganese oxide thin films were determined. Mixture of copper (II) chloride and manganese (II) chloride complexed ammonium hydroxide solution was used as precursor for cations. Sodium hydroxide placed in a hot plate at 60°C served as precursor for anions. Five samples of copper manganese oxide (CuMnO<sub>2</sub>) thin films were concurrently synthesized using 10 SILAR cycles to obtain desired thickness. After deposition, four of the deposited CuMnO<sub>2</sub> thin films were annealed at 473 K, 573 K, 673 K and 773 K respectively while one as-grown sample was used as a control. Thickness of deposited thin film estimated using gravimetric method increased as annealing temperature increases. Optical, structural, morphological, and elemental composition analysis were carried out on the samples. Optical results showed that annealing temperature has a significant effect on the optical properties. Structural analysis showed an improvement in the crystallinity of the films. Crystallite size of the deposited thin film obtained ranged between 14.36 nm – 33.14 nm. It was found that increase in annealing temperature resulted to increase in the crystallite sizes. SEM micrographs showed an increase in thin film particles and surface roughness as a result of increase in annealing temperature. Relative amounts of Cu, Mn and O<sub>2</sub> were found in the EDS results obtained.

## 1 Introduction

Ternary transition metal oxide (TTMO) thin films are set of material thin films that contain two transition metals and oxygen. They are formed when p orbital in oxygen connects with the half-filled and empty d orbitals of adjacent transition metal cations [1]. Copper manganese oxide is one of the promising TTMO due to its properties and applications in areas such as oxygen reduction reaction (ORR) [2], wettability and electrochromic performance [3], glucose sensitivity measurement [4], solar selective absorber [5-6], catalytic properties [7-11]. In the work, nanostructured copper manganese oxide thin film was deposited onto a microscopic

glass substrate by SILAR method. manganese ion was introduced in minute amount and effect of annealing temperature on the thickness, optical, structural, morphological, and compositional properties of the deposited copper manganese oxide were studied.

## 2 Materials and Methods

Copper manganese oxide thin films were deposited on a microscopic glass substrate using successive ionic layer adsorption reaction (SILAR) method. The SILAR approach used in this deposition was a four-step (made up of four beakers A, B, C and D) method. The four steps are cationic dipping (beaker A), rinsing with distilled water (beaker B), anionic

\* CORRESPONDING AUTHOR | N. L. Okoli | [okolinonsolivinus@gmail.com](mailto:okolinonsolivinus@gmail.com)

© The Authors 2022. Published by JNMSR. This is an open access article under the CC BY-NC-ND license.

dipping (beaker C) and finally rinsed in distilled water (beaker D). Reagents used for the deposition were molar solutions of copper (II) acetate monohydrate and manganese (II) chloride tetrahydrate as cationic precursors respectively. Sodium hydroxide solution was used as anionic precursor. 0.2 M of copper (II) acetate monohydrate and 0.05 M of manganese (II) chloride were used while 0.5 M of sodium hydroxide was used in the deposition.

One SILAR growth cycle with cycle time ( $t_c$ ) equals to 100 seconds shown in figure 1 involved four steps which are:

- (i) Cationic dipping: the cleaned substrate was immersed in first reaction bath containing 40 ml each of the solutions of 0.2 M of copper and 0.05 M of manganese precursors for 40 s. This process leads to absorption of  $\text{Cu}^{2+}$  and  $\text{Mn}^{2+}$  ions on the surface of the substrate.
- (ii) Rinsing: this involves rinsing the substrate with distilled water (DW) for 10 s to remove excess  $\text{Cu}^{2+}$  and  $\text{Mn}^{2+}$  ions that were loosely bounded to the glass substrate.
- (iii) Anionic dipping: The substrate was then immersed in freshly prepared sodium hydroxide solution placed in a hot

plate at 60°C for the 40 s. The oxygen ions ( $\text{O}^{2-}$ ) reacted with the absorbed  $\text{Cu}^{2+}$  and  $\text{Mn}^{2+}$  ions on the active center of the substrate to form copper manganese oxide films.

- (iv) Rinsing: Again, the substrate was rinsed in DW for 10 s to remove loosely bounded ions present on the substrate and unreacted  $\text{Cu}^{2+}$ ,  $\text{Mn}^{2+}$  and  $\text{O}^{2-}$  ions. The procedure was repeated for 10 cycles to get the desired uniform film with good thickness.

At the end of a cycle, uniform films of copper manganese oxide were seen on the surface of the microscopic glass substrate. Physical observation of the glass substrates showed thin films of relatively equal thickness because the five samples were found under the same growth conditions.

These deposited copper manganese oxide thin films were subjected to annealing treatment to determine the effect of annealing temperature on the properties of the films. First sample was left unannealed while four other samples were annealed at temperatures of 473 K (200°C), 573 K (300°C), 673 K (300°C) and 773 K (400°C) respectively.

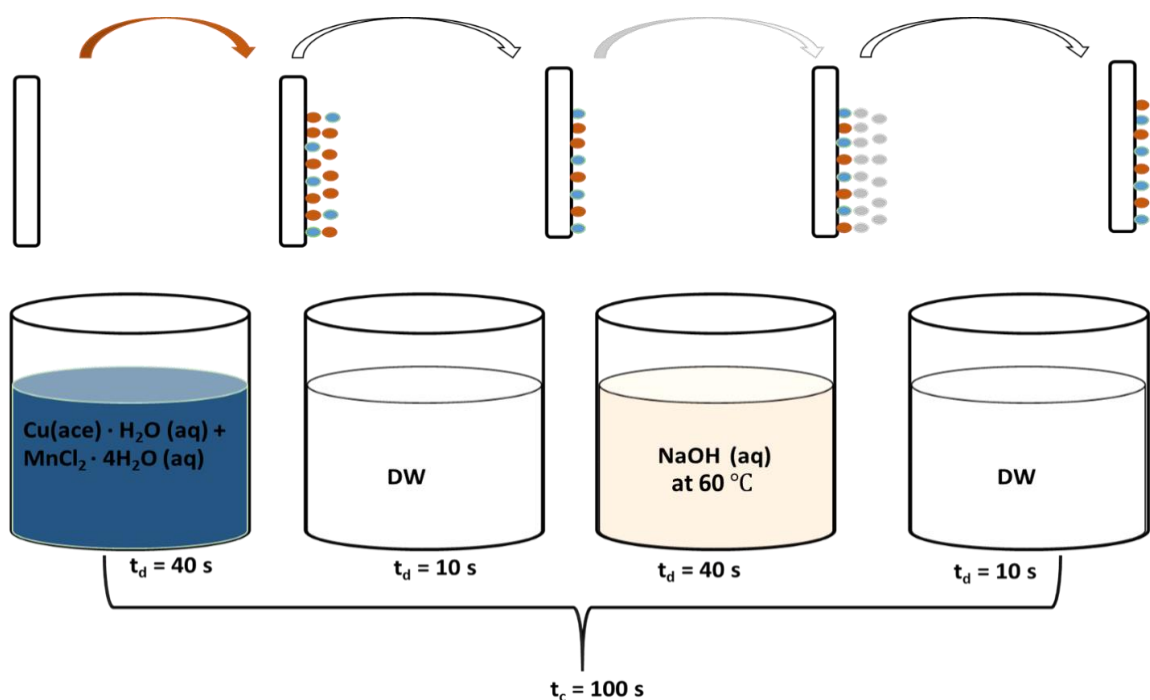


Figure 1: Schematic diagram of SILAR method for the deposition of copper manganese oxide thin films ( $\bullet \rightarrow \bullet$   $\text{Cu}^{2+}$ ,  $\bullet$   $\text{Mn}^{2+}$ ,  $\bullet$   $\text{O}^{2-}$ ): a)  $\rightarrow$  cationic precursors, b)  $\rightarrow$  ion exchange water, c)  $\rightarrow$  anionic precursor and d)  $\rightarrow$  ion exchange water,  $t_d \rightarrow$  dip time and  $t_c \rightarrow$  c

Deposited copper manganese oxide thin films were subjected to optical, structural, morphological and compositional characterizations. Thicknesses of the thin films were obtained using gravimetric techniques. Optical analysis was done using UV-VIS spectrophotometer (model: 756S UV-VIS) at Nano Research Laboratory, Department of Physics and Astronomy, University of Nigeria Nsukka, Enugu State, Nigeria. Structural

analysis was done using x – ray diffraction machine (Bruker D8 high resolution X-ray diffractometer) at Material Research Department, iThemba Labs, Johannesburg, South Africa. Morphological and compositional analyses of the films were done using the scanning electron microscope (MIRA TESCAN SEM) located at the Electron Microscope Unit, University of Cape Town, South Africa.

### 3 Results and Discussions

#### 3.1 Optical Analysis

Optical properties such as absorbance, transmittance, reflectance, extinction coefficient and optical band gap of the deposited thin films were studied within the electromagnetic wavelengths of 300 nm to 400 nm (ultraviolet: UV), 400 nm to 700 nm (visible light: VIS) and 700 nm to 1100 nm (near infrared: NIR).

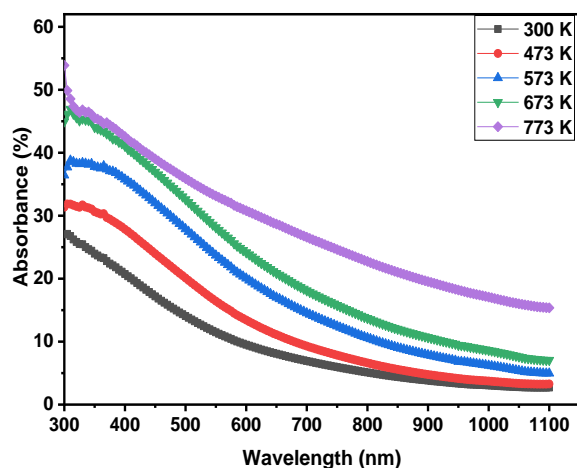


Figure 2: Plot of absorbance against wavelength for SILAR deposited copper manganese oxide thin films annealed at different temperature

Figure 2 showed the absorbance of copper manganese oxide films plotted against wavelength. Absorbance values of the films were found to decrease as wavelength increased from 300 nm to 1100 nm. It is also found to increase as annealing temperature increased.

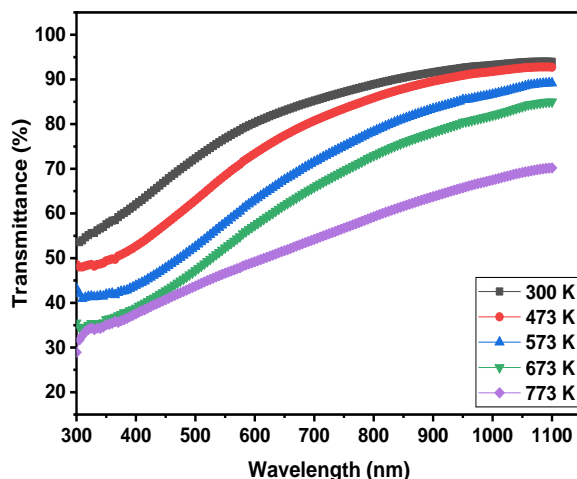


Figure 3: Plot of transmittance against wavelength for SILAR deposited copper manganese oxide thin films annealed at different temperature

Figure 3 showed the graph of transmittance spectra plotted against wavelength. Transmittance values of the films were

found to increase as wavelength increased from 300 nm to 1100 nm.

Secondly, the transmittance was found to decrease as annealing temperature increases. These set of films showed moderate transmittance values within UV with high transmittance values observed within VIS and NIR regions. The low transmittance of the films within UV region showed that they could be used as smart coating for heat mirrors.

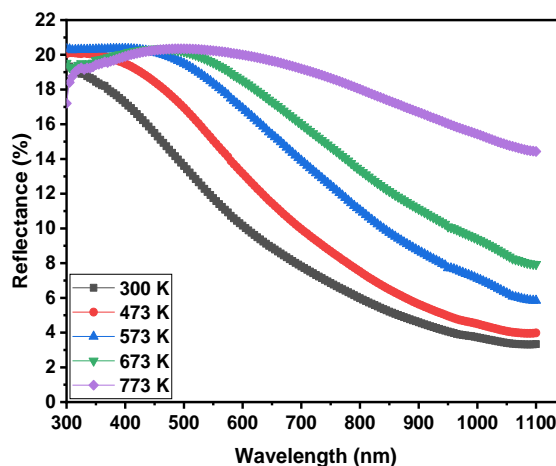


Figure 4: Plot of reflectance spectra against wavelength for SILAR deposited copper manganese oxide thin films annealed at different temperature

Figure 4 showed the graph of reflectance plotted against wavelength for SILAR deposited copper manganese oxide thin film annealed at different temperatures. The reflectance of the films is found to be low with peak value 20.35% observed within UV region and least value of 3.34% was observed within NIR region. Also, reflectance values decreased as wavelength increased from 400 nm within VIS region to 1100 nm in NIR regions.

Figure 5 showed the graph of extinction coefficient plotted against wavelength for SILAR deposited copper manganese oxide thin films. Extinction coefficient values was found to increase within UV region to peak values within VIS region before decreasing to their least values within NIR regions.

Except for film annealed at 773 K that has extinction coefficient which is different from others. The changes observed in the extinction coefficient spectra of film annealed at 773 K may be as a result of improved crystal structure.

Figure 6 showed the plot of refractive index against wavelength for SILAR deposited copper manganese oxide thin films. Refractive index of the films was found to be approximately the same within the UV region but decreased as wavelength increases towards VIS and NIR regions. The refractive index of the film was found to increase as annealing temperature increased. The films are of low reflectance with values ranged from 2.63 to 1.44.

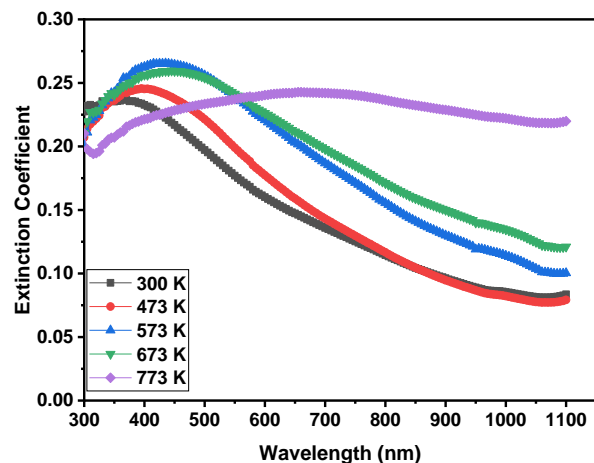


Figure 5: Plot of extinction coefficient against wavelength for SILAR deposited copper manganese oxide thin films annealed at different temperature

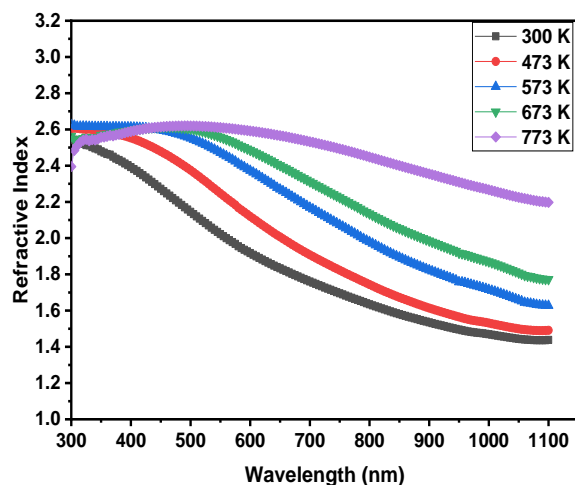


Figure 6: Plot of refractive index against wavelength for SILAR deposited copper manganese oxide thin films annealed at different temperature

Figure 7 showed the graph of  $(\alpha h\nu)^2 = 0$  plotted against photon energy for films copper manganese oxide thin films annealed at different. Energy band gap values of the films were estimated by extrapolating the straight portion of the graph along the photon energy axis where  $(\alpha h\nu)^2 = 0$ . Energy band gap of the films were found to range from 2.70 eV and 2.15 eV. This showed that the energy bad gap decreased as annealing temperature increases. The energy band gap values obtained are close to values reported by [3,12-13].

### 3.2 Film Thickness Measurement

Thickness of the deposited thin films was calculated using mass difference method according to [14-16] as given in equation (1):

$$t = \frac{\Delta m}{\rho A} \quad (1)$$

Where  $\Delta m$  is the mass difference of the films obtained by measuring the mass of the substrate before and after deposition,  $\rho$  is the bulk density of CuO which is 6.31 g/cm<sup>3</sup> and A is the area of substrate covered by the deposited thin films.

Figure 8 showed the graph of film thickness plotted against annealing temperature. From the figure, film thickness was found to increase as annealing temperature increased from 473 K to 773 K. This is due to the improvement in the crystalline nature of the deposited thin films as annealing temperature increases. As temperature increases, more ionic layers of copper manganese oxide were formed thereby increasing the thickness of the films. Annealing temperature was also found to affect the band gap of the deposited thin films. Energy band gap was found to decrease as annealing temperature increases.

### 3.3 Morphological Properties

Figure 9 showed the SEM micrographs of the deposited thin films revealing the surface structure of the thin film. These micrographs showed that the surfaces of the thin films are made up of nanostructured particles of different sizes and shapes. Improvement in the surface morphology of the deposited copper manganese oxide thin films was observed as annealing temperature increased 573 K to 773 K.

### 3.4 Compositional analysis

Figure 10 showed the energy dispersive x – ray spectroscopy (EDS) spectra of copper manganese oxide thin films deposited at 300 K and those annealed at 573 K and 773 K. The EDS spectra showed the presence of the desired elements of copper manganese and oxygen. Traces of other elements were observed which are likely as a result of elemental compositions of the microscopic glass substrates.

The EDS spectra showed that the atomic percentages of copper, manganese increased as annealing temperature increases. Atomic percentage of oxygen was found to increase as temperature increases. This increase in oxygen content may be as a result of oxidation of the films at higher temperature.

### 3.5 Structural properties

Structural analysis of SILAR deposited copper manganese oxide thin films were carried out using diffractometer (Bruker D8 advance diffractometer). The XRD results for the deposited thin films of copper manganese oxide are presented in figure 11. The XRD spectra obtained showed peaks corresponding to CuO, Mn<sub>3</sub>O<sub>4</sub> and spinel Cu<sub>1.5</sub>Mn<sub>1.5</sub>O<sub>4</sub>.

The XRD spectra of as-deposited (300 K) copper manganese oxide thin film showed peaks at 35.58°, 38.72° and 48.78° which correspond to monoclinic phase of copper oxide of mineral name tenorite with JCPDS file number of 00-45-0937. Film annealed at 573 K showed the formation of mixed oxides of copper and manganese. In addition to peaks observed in as-deposited (300 K) thin films, new peaks at 32.41° and 44.37° were observed. These peaks were attributed to tetragonal phase of manganese oxide (Mn<sub>3</sub>O<sub>4</sub>) with JCPDS file number of 00-018-0803.

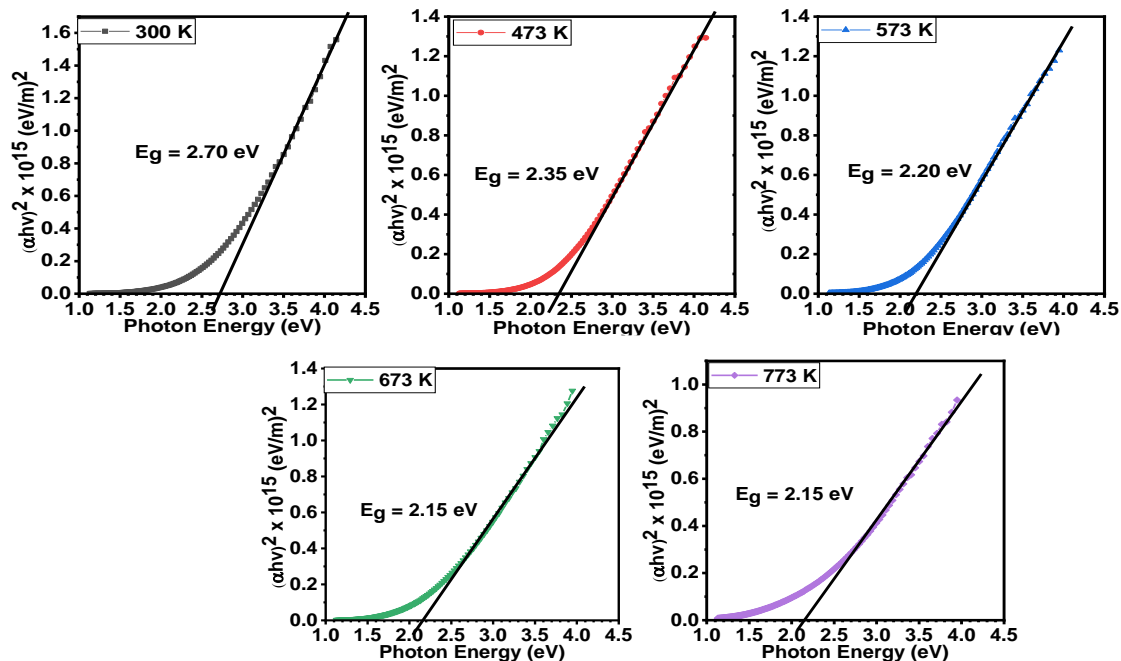


Figure 7: Plot of  $(\alpha h\nu)^2$  against photon energy ( $h\nu$ ) for SILAR deposited copper manganese oxide thin films annealed at different temperature

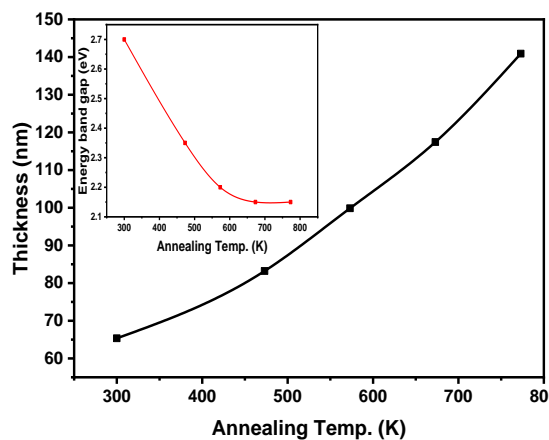


Figure 8: Plot of thickness (nm) against annealing temperature for SILAR deposited copper manganese oxide thin films and variation of energy band gap with annealing temperature

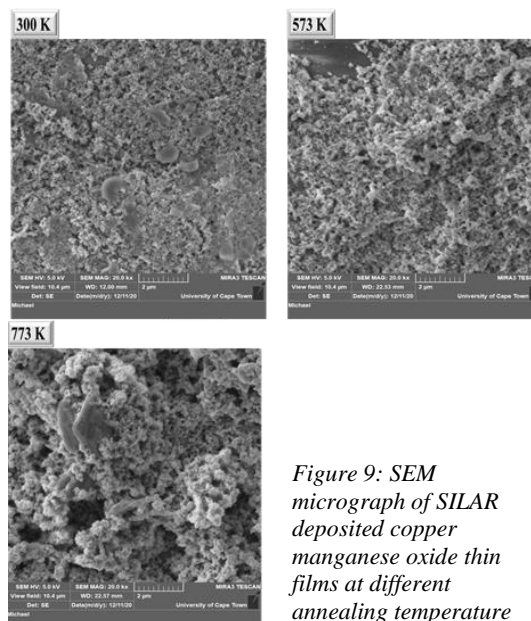


Figure 9: SEM micrograph of SILAR deposited copper manganese oxide thin films at different annealing temperature

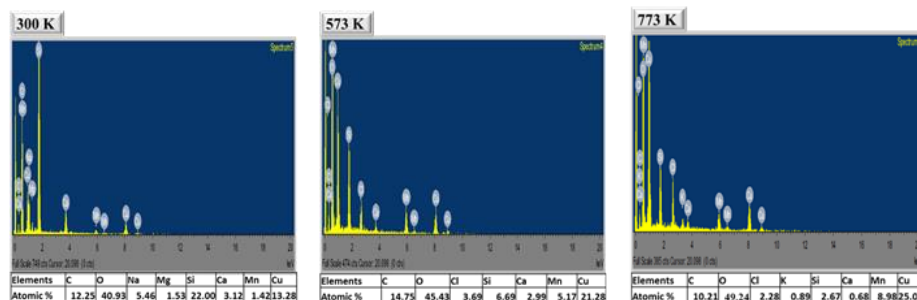


Figure 10: EDS spectra of SILAR deposited copper manganese oxide thin films



Film annealed at 773 K showed two additional peaks at  $57.81^\circ$  and  $63.86^\circ$  which were attributed to cubic spinel structural phase of copper manganese oxide with formula  $\text{Cu}_{1.5}\text{Mn}_{1.5}\text{O}_4$  corresponding to JCPDS file number of 01-070-0260. These results showed the formation of copper manganese oxide structure at 773 K though the peaks attributed to  $\text{Cu}_{1.5}\text{Mn}_{1.5}\text{O}_4$  are weak compared to peaks observed for  $\text{CuO}$  and  $\text{Mn}_3\text{O}_4$ . Formation of  $\text{Mn}_3\text{O}_4$  at 573 K is in line with report of [17].

Also, similar results of formation of copper oxide, manganese oxide and copper manganese oxides have been reported by [8, 9, 19, 20]. Crystallite sizes of the films were obtained using Debye-Scherrer's relation in equation (2) as given by [21, 22, 23].

Other structural parameters such as dislocation density and micro-strain were calculated using equations (3) and (4) respectively [24, 25].

$$D = \frac{k\lambda}{\beta \cos \theta} \quad (2)$$

$$\delta = \frac{1}{D^2} \quad (3)$$

$$\varepsilon = \frac{\beta}{4 \tan \theta} \quad (4)$$

where  $\lambda$  = wavelength,  $\beta$  = full width at half maximum (in radians) and  $\theta$  = the angle of diffraction. Crystallite size of the films was found to be 14.36 nm, 24.50 and 33.14 nm. Increase in annealing temperature was found to cause an increase in the crystallite size of the deposited thin film. Dislocation densities of the films were found to be  $4.78 \times 10^{15}$  lines/m<sup>2</sup>,  $1.85 \times 10^{15}$  lines/m<sup>2</sup> and  $1.77 \times 10^{15}$  lines/m<sup>2</sup> while values of the micro-strain of the films were found to be  $7.30 \times 10^{-3}$ ,  $4.57 \times 10^{-3}$ , and  $4.04 \times 10^{-3}$ . Dislocation density and micro-strain were found to decrease as annealing temperature increased from 300 K to 773 K.

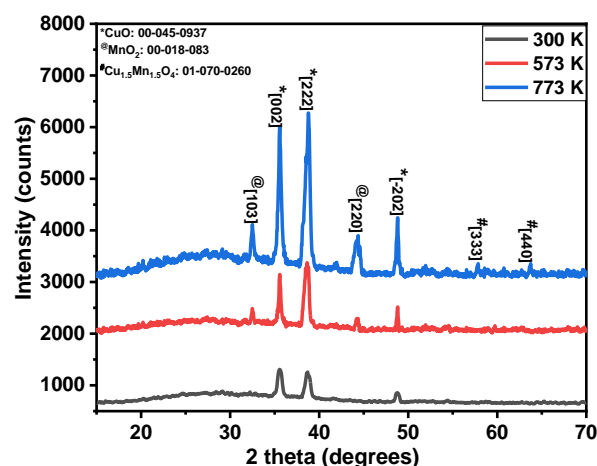


Figure 11: XRD spectra SILAR deposited copper manganese oxide thin films

## 4 Conclusion

Nanostructured copper manganese oxide thin films deposited by SILAR method were studied. The deposited thin films were annealed at different temperatures of 473 K, 573 K, 673 K and 773 K respectively with one of the samples kept as-deposited (unannealed) at 300 K. The thickness, optical, structural, morphological, and compositional properties of the films were carried out using appropriate equipment. The thickness values of 65.34 nm to 140.91 nm showed that the deposited copper manganese oxide thin film layers are nanostructured. Optical properties showed that the thin film layers have high absorbance and low transmittance within UV; and low absorbance and high transmittance within VIS – NIR region. The highest transmittance values were observed within NIR region for all the films while the energy band gap values of the films were found to be between 2.70 eV and 2.15 eV. The structural analysis showed the formation of copper oxide and spinel phase of copper manganese oxide. The spinel phase of the films was obtained at higher annealing temperature of 773 K. Crystallite sizes of deposited thin film ranged between 14.36 nm and 33.14 nm. Micrograph images showed that the films are made of nanostructured particles of different sizes and shapes while the compositional analysis revealed the presence of copper, manganese, and Oxygen. The films are found to be rich in oxygen. These results showed that annealing temperature could be used to modify film thickness, optical, structural, morphological, and compositional properties of copper manganese oxide thin film layer.

## Acknowledgment

We appreciate the contributions made by the staff of Nano Research Group, University of Nigeria Nsukka, Enugu State, Nigeria and Electronic Microscopic unit, University of Cape Town, South Africa by providing access to instruments for analyses of the samples.

## Declaration of Competing Interest

Authors have declared that there was no conflict of interest.

## References

- [1] Abdulvagidov, S.B., Djabrailov, S.Z. and Abdulvagidov, B. S. (2019). Nature of novel criticality in ternary transition-metal oxides. *Sci Rep* 9, 19328. DOI: <https://doi.org/10.1038/s41598-019-55594-w>
- [2] Toh, R.J., Eng, A.Y.S., Sofer, Z., Sedmidubsky, D. and Pumera, M. (2015). Ternary Transition Metal Oxide Nanoparticles with Spinel Structure for the Oxygen Reduction Reaction. *CHEMELECTROCHEM*, 2: 982-987. DOI: <https://doi.org/10.1002/celc.201500070>
- [3] Falahatgar, S. S., Ghodsi, F. E., Tepehan, F. Z., Tepehan, G.G., Turhan, I. (2014). Electrochromic performance, wettability and optical study of copper

- manganese oxide thin films: Effect of annealing temperature. *Applied Surface Science*, 289, 289–299 DOI: <https://doi.org/10.1016/j.apsusc.2013.10.153>
- [4] Zahan, M. and Podder, J. (2020). Structural, optical and electrical properties of Cu:MnO<sub>2</sub> nanostructured thin films for glucose sensitivity measurements. *SN Applied Science*, 2, 385, DOI: <https://doi.org/10.1007/s42452-020-2191-8>
- [5] Ma, P., Geng, Q., Gao, X., Yang, S. and Li, G. (2016). Aqueous chemical solution deposition of spinel Cu<sub>1.5</sub>Mn<sub>1.5</sub>O<sub>4</sub> single layer films for solar selective absorber. *RSC Advances*, 6, 54820-54829. DOI: <https://doi.org/10.1039/C6RA08777A>
- [6] Pal, S., Diso, D., Franza, S., Licciulli, A. and Rizzo, L. (2013). Spectrally selective absorber coating from transition metal complex for efficient photothermal conversion. *Journal of Materials Science*, 48(23), 8268 – 8276. DOI: <https://doi.org/10.1007/s10853-013-7639-4>
- [7] Yang, X. and Zhang, Z. (2021). Study on the Performance of Copper-manganese Composite Oxide Catalysts for Toluene. *ChemistrySelect*, 6(19), 4837 – 4843. DOI: <https://doi.org/10.1002/slct.202100945>
- [8] Wang, Y., Yang, D., Li, S., Zhang, L., Zheng, G. Guo, L. (2019). Layered copper manganese oxide for the efficient catalytic CO and VOCs oxidation. *Chemical Engineering Journal*, 357, 258-268. DOI: <https://doi.org/10.1016/j.cej.2018.09.156>
- [9] Chen, S., Tang, W., He, J., Miao, R., Lin, H., Song, W., Wang, S., Gao, P. and Suib, S. L. (2018) copper manganese oxide enhanced nanoarray-based monolithic catalysts for hydrocarbon oxidation. *Journal of Materials Chemistry A*, 6(39), 19047 – 19057. DOI: <https://doi.org/10.1039/C8TA06459H>
- [10] Clarke, T. J., Davies, T. E., Kondrat, S. A. and Taylor, S. H. (2015). Mechanochemical synthesis of copper manganese oxide for the ambient temperature oxidation of carbon monoxide. *Applied Catalysis B: Environmental*, 165, 222-231. DOI: <https://doi.org/10.1016/j.apcatb.2014.09.070>
- [11] Einaga, H., Kiya, A., Yoshioka, S. and Teraoka, Y. (2014). Catalytic properties of copper manganese mixed oxides prepared by coprecipitation using tetraammonium hydroxide. *Catalysis Science Technology*, 4(10), 3713-3722. DOI: <https://doi.org/10.1039/C4CY00660G>
- [12] Gülen, Y., Bayansal, F., Şahin, B., Çetinkara, H. A., & Güder, H. S. (2013). Fabrication and characterization of Mn-doped CuO thin films by the SILAR method. *Ceramics International*, 39(6), 6475–6480. DOI: <https://doi.org/10.1016/j.ceramint.2013.01.077>
- [13] Rahaman, R., Sharmin, M. and Podder, J. (2022). Band gap tuning and p to n-type transition in Mn-doped CuO nanostructured thin films. *Journal of Semiconductors*, 43(1), 1-11. DOI: <https://doi.org/10.1088/1674-4926/43/1/012801>
- [14] Ezenwaka, L. N.; Umeokwonna, N.S.; Okoli, N.L. (2020). Optical, structural, morphological, and compositional properties of cobalt doped tin oxide (CTO) thin films deposited by modified chemical bath method in alkaline medium, *Ceramics International*, 46(5), 6318-6325, DOI: <https://doi.org/10.1016/j.ceramint.2019.11.106>.
- [15] Nwanya, A. C., Obi, D., Osuji, R. U., Bucher, R., Maaza, M. and Ezema, F. I. (2017). Simple chemical route for nanorod-like cobalt oxide films for electrochemical energy storage applications. *Journal of Solid State Electrochemistry*, Volume 21(9), 2567 – 2576. DOI: <https://doi.org/10.1007/s10008-017-3520-8>
- [16] Ezenwaka, L. N., Okoli, N. L., Okereke, N. A., Ezenwa, I. A. and Nwori, N. A. (2021). Properties of Electrosynthesized Cobalt Doped Zinc Selenide Thin Films Deposited at Varying Time. *Nanoarchitectonics*, 3(1), 1 – 9. DOI: <https://doi.org/10.37256/nat.3120221040>
- [17] Augustin, M., Fenske, D., Bardenhagen, I., Westphal, A., Knipper, M., Plaggenborg, T., Kolny-Olesiak, J. and Parisi, J. (2015). Manganese oxide phases and morphologies: A study on calcination temperature and atmospheric dependence. *Beilstein Journal of Nanotechnology*, 6, 47–59. DOI: <https://doi.org/10.3762/bjnano.6.6>
- [18] Marin Figueredo, M. J., Andana, T., Bensaid, S., Dosa, M., Fino, D., Russo, N., & Piumetti, M. (2020). Cerium–Copper–Manganese Oxides Synthesized via Solution Combustion Synthesis (SCS) for Total Oxidation of VOCs. *Catalysis Letters*, 150, 1821–1840. DOI: <https://doi.org/10.1007/s10562-019-03094-x>
- [19] Pal, R. and Basu, S. (2017). Low temperature synthesis of copper manganese oxide – polyaniline composite: Electrochemical characterizations for oxygen reduction reaction in acid media. *Ferroelectrics*, 519(1), 90–99. DOI: <https://doi.org/10.1080/00150193.2017.1361220>
- [20] Fan, F., Wang, L., Wang, L., Liu, J., & Wang, M. (2022). Low-Temperature Selective NO Reduction by CO over copper-manganese Oxide Spinels. *Catalysts*, 12(6), 1-12. DOI: <https://doi.org/10.3390/catal12060591>
- [21] Obodo, R. M., Mbam, S. M., Nsude, H. E. Ramzan, M., Ezike, S. C., Ahmad, I., Maaza, M. and Ezema, F. I. (2022). Graphene oxide enhanced Co<sub>3</sub>O<sub>4</sub>/NiO composite electrodes for supercapacitive devices applications. *Applied Surface Science Advances* 9(100254), 1-9. DOI: <https://doi.org/10.1016/j.apsadv.2022.100254>
- [22] Egwunyenga, N. J., Onuabuchi, V. C., Okoli, N. L. and Nwankwo, I. E. (2021). Effect of SILAR cycles on the

- thickness, structural, optical properties of cobalt selenide thin film. *International Research Journal of Multidisciplinary Technovation*, 10, 1-9. DOI: <https://doi.org/10.34256/irjmt2141>
- [23] Nsude, H. E., Obodo, R. M., Obodo, K. U., Ikhioya, L. I., Asogwa, P. U., Osuji, R. U., Maaza, M. and Ezema, F. I. (2022). Binder-free fabricated CuFeS<sub>2</sub> electrodes for supercapacitor applications. *Material Research Express*, 9(025501), 1-9. DOI: <https://doi.org/10.1088/2053-1591/ac4f13>
- [24] Awada, C., Whyte, G. M., Offor, P. O., Whyte, F. U., Kanoun, M. B., Goumri-Said, S., Alshoaibi, A., Ekwealor, A. B. C., Maaza, M. and Ezema, F. I. (2020). Synthesis and Studies of Electro-Deposited Yttrium Arsenic Selenide Nanofilms for Opto-Electronic Applications. *Nanomaterials*, 10(8), 1-15. DOI: <https://doi.org/10.3390/nano10081557>
- [25] Ezenwaka, L. N., Nwori, N. A., Ottih, I. E., Okereke, N. A. and Okoli, N. L. (2022). Investigation of the Optical, Structural and Compositional Properties of Electrodeposited Lead manganese Sulfide (PbMnS) Thin Films for Possible Device Applications. *Nanoarchitectonics*, 3(1):18-32. DOI: <https://doi.org/10.37256/nat.3120221226>